Validation of 3D turbulent CFD modelling of retrofitting works ventilation with experimental measurements for a rail tunnel

Nicolas A. Tonello[1], Elisa Béraud[2], Yohann Eude[1]
[1]Renuda, 329-339 Putney Bridge Road, London SW15 2PG, UK
[2]SNCF RÉSEAU, 15 rue Jean-Philippe Rameau, 93212 La Plaine St Denis Cedex, France

Abstract

To help plan the regeneration work required on its historic tunnels, SNCF Réseau has been developing increasingly sophisticated numerical tools. A validation study is presented based on measurements and 3D CFD simulations of the ventilation of the Grand Pissy-Poville tunnel during works. The sensitivity to train shape and tunnel wall characteristics is ascertained by comparing the measured and numerical values. However further atmospheric data would be required to improve the prediction throughout the entire tunnel. Good agreement can be obtained in the works area, indicating that the models developed can form the basis of future smoke and dust simulations.

1 INTRODUCTION

In underground sites, the airborne pollution generated by the building activities tends to accumulate, which could lead to concentrations exceeding safe limits for workers. Ensuring acceptable air quality is, therefore, a primary concern for tunnel works. This is achieved, firstly, by limiting emissions and, secondly, by ensuring continuous air movement through the tunnel to dilute or evacuate gas and dust pollution. In preparation of construction work in railway tunnels, worksite ventilation must be studied and, when natural ventilation is not sufficient, mechanical ventilation must be planned.

For simple tunnel shapes, SNCF Réseau uses a 1D model to evaluate the characteristics of the fans required to decrease concentration of exhaust gases generated by all the machinery. The 1D prediction tool is parametrised with coefficients which can be estimated for known shapes (1) and based on experience (2). This method has the advantage of giving good results in few minutes.

However, for more complex tunnel shapes with side openings or underground stations with network connections, and in the presence of irregular obstruction such as caused by engines and trains, coefficients are multiplied and airflow estimates with 1D modelling become difficult or inaccurate. Therefore, SNCF Réseau has been gradually developing 3D CFD models to perform ventilation estimations of these more complex scenarios. Whilst they make it possible to predict ventilation in complex building situations, these 3D methods must nonetheless remain practical, both in terms of computational time and in terms of expertise of the modellers. In addition and particularly because they are used for health and safety decisions, before their adoption can be generalised, they must be understood, validated, and calibrated.

This paper presents the results of a detailed validation study performed on the Grand Pissy-Poville tunnel by comparing numerical results for different CFD models to experimental measurements obtained during night time regeneration work on the tunnel.

The French railway context, including the specificities of the network, tunnels, and regulations is presented first. Then, the measurements campaign and the experimental results are described, followed by details of the numerical models, and a comparison and analysis of the numerical and experimental results.

2 CONTEXT

2.1 The French railway network

In January 2015, SNCF Réseau became the single owner and operator of the French railway network. It is responsible for maintaining, upgrading and updating the infrastructure, optimizing the allocation of train routes on the network, and selling access to the network for all passenger and freight transport companies. This involves managing about 30,000 km of tracks, including 2,700 km of high-speed tracks (with the opening of the SEA/Oceane and BPL lines in the summer 2017), 15,000 daily trains (passengers and freight), 5 million passengers per day, 250,000 tonnes of merchandise, and allocating 7 million rail routes each year.

Part of the infrastructure is over 100 years old and represents a national heritage. The vast majority of the 1,380 active tunnels of the French railway network was built in the 19th century. Because of their age, the tunnels may be affected by different pathologies, ranging from changes in the surrounding terrain (mechanical origin) to ageing of the tunnel lining materials (physical/chemical phenomena). As a consequence, regeneration work is regularly conducted on the structures (3).

2.2 Maintenance of the French railway tunnels

Interventions in tunnels are subject to stringent constraints. Whilst, in some instances, work can be carried out on one track whilst trains are still running on the other track, most of the time traffic is stopped on both tracks. This can involve closing the entire line during a period of time for concentrated bursts of activity, or closing the line at night only, carrying out the work over several weeks. In this configuration, work is limited to short, 4-6 hours periods between the last evening train and the first train the following day. To make the most of this limited timeframe, work is distributed over multiple workstations, often resulting in a large quantity of equipment occupying the tunnel, operating simultaneously and causing pollution.

As the exhaust gases from the machines and the dust generated can cause health and safety risks for workers, in France the safe thresholds are regulated in the Labour Code

and in circulars issued by the Ministry of Employment. For gaseous species, the maximum allowable concentrations are specified by the short-term (VLCT-15 min) and the time-weighted average (VLEP-8 hrs) limit exposure values. Similar to the TLV-STEL, the VLCT specifies the maximum concentration in the air to which an individual may be exposed over a 15 minutes period without health risks. VLEP is equivalent to TLV-TWA and specifies the maximum, average concentration to which a person may be exposed without risk during an eight-hour shift. This threshold may be exceeded for short durations, provided the maximum limit value is not exceeded. If the thresholds are exceeded, work must stop, potentially leading to delays and further complications.

To minimise these risks, the concentration of pollutants in the tunnel is actively maintained below the legal thresholds by creating an air flow through the tunnel. Hence, a ventilation system is required, which must be specifically designed for each work site and adapted to the tunnel in compliance with the AFTES's (French Tunnelling and Underground Space Association) code of practice (4)(5).

2.3 Ventilation for the French underground rail worksites

In the AFTES GT27 recommendations, the minimum required flow rate is evaluated for three objectives: personnel breathing requirements, dilution of gases, and dust removal. The largest of the three values is then retained to dimension the ventilation. In the presence of the powerful locomotives needed to move the building trains into the tunnel, the required flow rate of 50 l/s per effective horsepower (HP) is often the dimensioning factor compared to the other two values (6).

For rail tunnels, which are open at both ends, AFTES recommends ventilating by extracting air from the tunnel. Whilst this can sometimes be achieved solely by the air currents that occur naturally within the tunnel, often additional forced ventilation is required. Temporary fan units installed on stands or building trains are then positioned in a way compatible with the progress of the worksite. They are removed at the end of each work shift to free the tunnel for scheduled rail traffic.

2.4 Regeneration work: the example of Pissy-Poville

The Grand Pissy-Poville tunnel was chosen as a validation test case as it represents a typically complex case of a historical tunnel and a test campaign could be conducted during recent, large regeneration works aimed at adding strengthening spars and sprayed concrete which involved 50 people working at night over 12 months.

Situated on the East-West, Paris to Le Havre route, between kilometre markers 150 and 153, the Grand Pissy-Poville tunnel is 2,210 metre long and includes three ventilation shafts situated at the metric markers 731, 1604, 1970 (from the Paris (East) portal). It is followed 100 metres away to the West by the smaller Petit Pissy-Poville tunnel which also underwent strengthening and resurfacing work but is not taken into account in the measurements and simulations.

For these works, mechanical ventilation was required to help evacuate exhaust gases from combustion engine machinery, such as locomotives and electricity generators, and dust particulates which could not be contained, for example those discharged from the concrete spraying stations. Two individual fan systems were installed on rail cars and inserted into the tunnel as part of two separate building trains.

On the night of the campaign, four building trains were located between the East entrance and the first ventilation shaft of the tunnel, as schematised in Fig. 1 below.

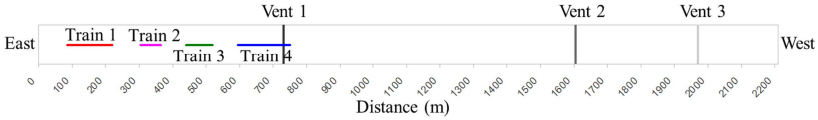

Figure 1: Positions of the building trains inside the tunnel the night of the measurements.

The four trains were configured with different systems, including locomotive or pusher cars, concrete supply cars, cars with electric generators, elevating platforms, mini-excavators, a rubble collection car and a car with living quarters.

Photographs of train 4 taken the night of the measurements are presented in Fig. 2 below.

(a): Traction engine

(b) Ventilation fan car

(c): Elevation platform

(d): Rubble collection car

Figure 2: Photographs of train 4 taken the night of the measurement campaign.

3 MEASUREMENT CAMPAIGN

The measurements campaign was performed by the AEF (Agence Essais Ferroviaires, or Railway Test Agency) laboratory of SNCF (www.eurailtest.com), the organisation responsible for testing, appraisals and commissioning of rolling stock, as well as physico-chemical analyses, materials appraisals and failure analyses, industrial hygiene, chemical hazards, fire behaviour, etc.

Flow velocity measurements were performed in order to provide data for validation of the numerical models. Gas concentration measurements were also carried out in order to verify that the ventilation had been dimensioned correctly and was adequate.

3.1 Protocol

Due to worksite constraints, it was only possible to carry out measurements at 6 different locations, distributed in the four sections of the tunnel delimited by the ventilation shafts. The measurement planes were situated 410, 920, 1200, 1400, 1800 and 2100 m from the tunnel entrance. Their position is represented as P1 to P6 on the diagram of Fig. 3 below, along with the position of the different building trains at the time of the measurements.

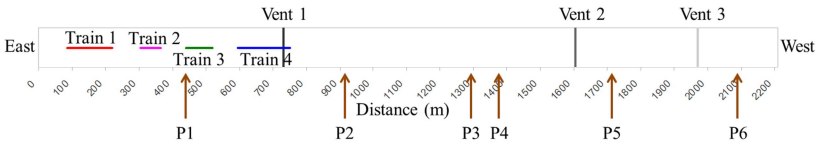

Fig. 3: Schematic of the position of the building trains and the measurement planes.

Two series of simultaneous measurements at different planes were carried out. The first one at planes 1, 3 and 5, and the second one at planes 2, 4 and 6.

The mean, minimum and maximum flow velocity was measured using tripod mounted KIMO AMI 310 windmill anemometers (Fig. 4(a)), which can handle a velocity range of 0.3 to 20m/s.

(a) Anemometer during the flow velocity measurements.

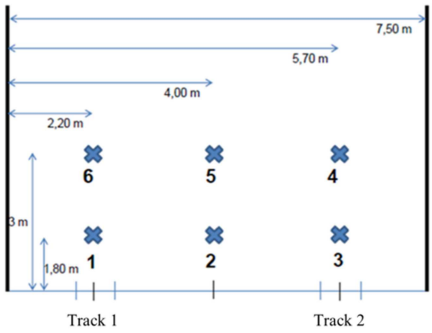

(b) Distribution of the measuring points in each measuring plane.

Figure 4: Flow velocity measurements protocol.

Six measuring points (Fig. 4(b)) were used in each measuring plane, corresponding to a point in the middle of each railway track and a point between the two tracks, at two different heights (1.8 m and 3.0 m). For each point, the flow velocity was recorded with a frequency of 10 secs and averaged over a 3 mins period. This methodology made it possible to record measurements at 36 different locations.

Gas concentration measurements were also performed for carbon monoxide (CO), nitrogen monoxide (NO) and nitrogen dioxide (NO_2) using Miniwarn instruments, which were set to continuously record and average the concentrations over 10 seconds periods. The gas concentrations were recorded next to the propeller of the anemometers at the velocity measurement points and, in addition, next to the first trains' locomotives. The gas concentration measurements recorded to verify air quality on the work site could be used in future validation studies of simulations taking into account smoke and dust and are not presented further.

3.2 Results – Mean Velocity

Table 2 presents the measured values of velocity at each measuring point and each measuring plane.

Table 2: Measured, mean velocity magnitude at each measuring plane and point within each plane. In m/s.

	Measuring Plane					
Point	**P1**	**P2**	**P3**	**P4**	**P5**	**P6**
1	2.93	2.25	2.07	2.11	1.26	0.80
2	2.96	2.23	2.30	2.34	1.42	0.69
3	3.17	2.29	1.85	2.02	1.29	0.70
4	3.30	2.36	2.18	2.28	1.51	0.81
5	3.13	2.42	2.38	2.53	1.38	0.82
6	2.99	2.60	2.19	2.34	1.38	0.86

To evaluate the ventilation in the tunnel, the minimum, maximum and the mean between these two values are extracted and plotted along the tunnel length (Fig.5).

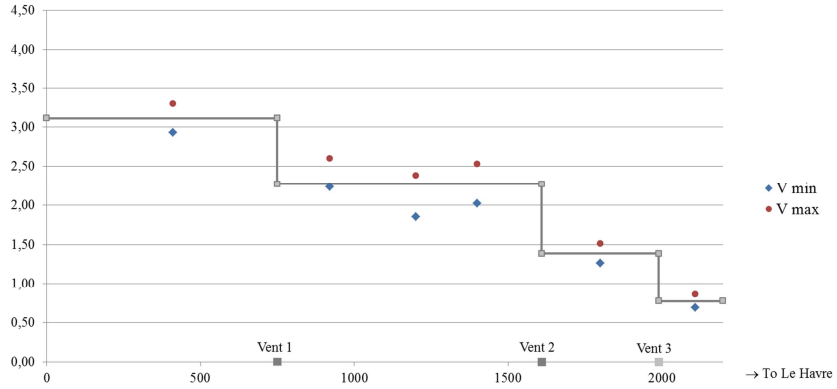

Figure 5: Min, max, and mean measured velocities along the tunnel length.

The position of the ventilation shafts is indicated by the grey squares on the horizontal axis. The graph shows that the velocity decreases significantly between the shafts,

highlighting their importance in the ventilation of the tunnel. The fans ensure that the velocity magnitude is of the order of the required threshold of 3m/s in the first section, where the building trains and workers are situated.

4 NUMERICAL MODELLING

4.1 Software and hardware tools

The numerical study was realised entirely using open source software tools and a 12 cores workstation with 128GB of RAM. The geometry creation was carried out using the GEOM module of the SALOME platform (7). The mesh was built using the *snappyHexMesh* utility and the Navier-Stokes equations were solved using the *simpleFoam* solver, both part of the OpenFOAM CFD software toolbox (8). Flow visualisation and analysis was performed using Paraview (9).

4.2 Computational domain

The geometry of the tunnel (Fig. 6) was built from plans and included all three ventilation shafts. Safety cells were also included, with all other internal geometric details on a smaller scale such as the tracks, catenary wires, or the ballast removed and represented by surface roughness heights.

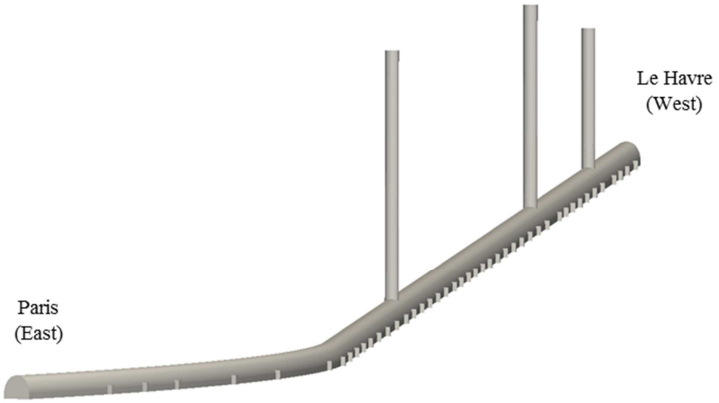

Figure 6: CAD model of the Grand Pissy-Poville tunnel.

Inlet/outlet boundary conditions are applied at each end of the tunnel and at each ventilation shaft. For natural ventilation, a pressure differential of 5.5Pa is applied between the tunnel entrance and exit. The value is taken from a rough 1D estimate corresponding to about 1m/s of natural ventilation in the tunnel, or 30% of the estimated required flow for proper ventilation. In the calculations with both forced and natural ventilation, as a worst case scenario the pressure gradient is imposed in the direction opposite of the air blown by the fans.

4.3 Physical and numerical model

The air is considered to be incompressible, with fixed properties. Temperature variations are not taken into account. The Navier-Stokes equations are solved in 3D, supplemented by the RANS, k-ω SST high-Re model to account for turbulence. The calculations are conducted with the SIMPLE, stationary algorithm and second-order spatial accuracy.

4.4 Sensitivity Study Parameters

In order to establish guidelines, three parameters were selected for variation: train shape, surface roughness, and ventilation.

4.4.1 Building trains

Two different types of geometries were created for the trains. The first one (Fig. 7a), described as 'tubular', has the overall dimensions of the trains but no features aside from the ventilation fan and its car. The second one (Fig. 7b) is detailed with individual locomotives and cars, and shapes of representative of car loads.

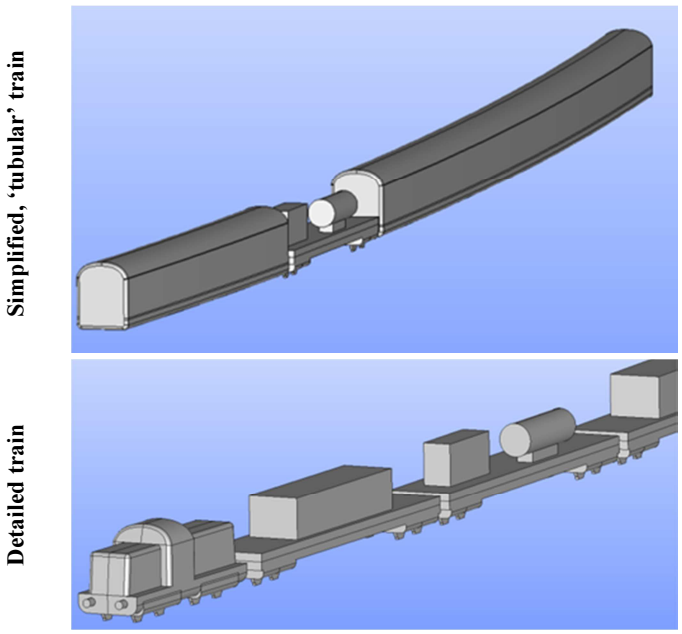

Figure 7: CAD of the tubular and detailed train models.

4.4.2 Surface roughness

Cases are compared with and without surface roughness. When surface roughness is modelled, different surface roughness heights are used to represent bricks (5mm), sprayed concrete (1cm) and the track ballast (3cm). The position of the different types of surfaces are taken directly from the tunnel plans: sprayed concrete from 0 to 490m, bricks up to 900m, sprayed concrete from 900m to 1610m, bricks up to 2000m, and finally sprayed concrete to the end of the tunnel (2209m).

4.4.3 Ventilation

Different scenarios are studied, with and without natural ventilation, and with forced ventilation. The actual power settings for the fans the night of the measurements were not known. For the parametric study of the surface roughness and train shape, they were assumed to be blowing at maximum power on train 1 ($60.32 m^3/s$) and train 4 ($95.1 m^3/s$). This setting was then modified to evaluate its influence on the results, as discussed in Section 5.3.

4.5 Meshes

Hexahedral dominant meshes were created for the different cases with wall layers adapted to ensure that $30 < y^+ < 300$ for each case. Views of the surface and volume meshes are shown in Figs. 8 and 9 below for illustration.

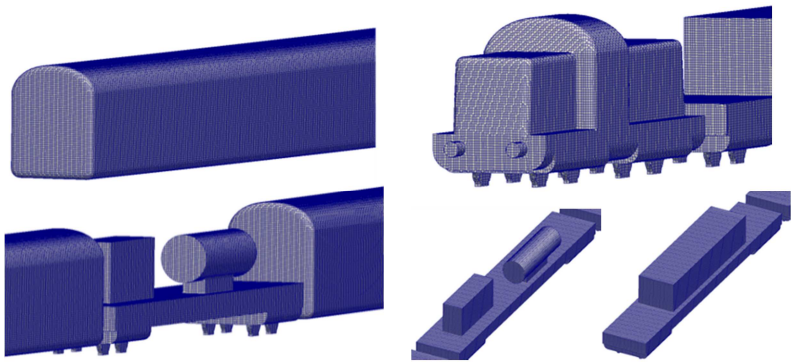

(a) 'Tube' train model (b) Detailed train model

Figure 8: Views of the surface mesh for the two train models.

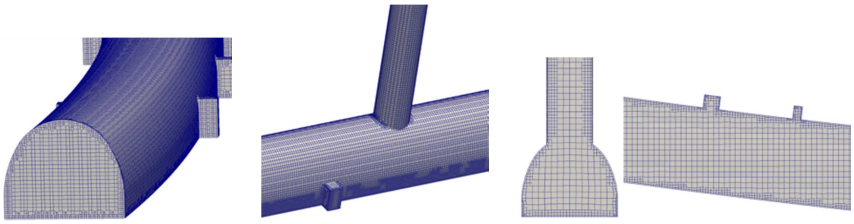

Figure 9: Views of the tunnel surface and volume mesh.

The meshes contained between 13.3 and 13.8 million cells.

5 RESULTS AND ANALYSIS

Two series of calculations were performed. The first one to evaluate natural ventilation and its modelling in the tunnel, and the second, the parametric study on the train's shape and tunnel surface roughness.

5.1 Natural Ventilation

Field data for ventilation inside the tunnel in absence of trains or fans was not available. However, as it could be an important parameter to consider in addition to the forced ventilation, a first series of calculations was conducted to evaluate the flow field inside the tunnel under assumed natural ventilation conditions. For these runs, a pressure differential of 5.5 Pa was applied between the tunnel entrance and exit, taken from a rough 1D estimate corresponding to about 1m/s of natural ventilation in the tunnel, or 30% of the estimated required flow for proper ventilation. Three different models were examined, keeping the same pressure gradient but specifying the pressure boundary conditions from East to West as 0.0 to 5.5 Pa, -2.75 to 2.75 Pa, and -5.5 to 0 Pa.

A comparison between the three calculations shows that the way the pressure gradient to simulate natural ventilation is specified has a large influence on the flowfield. This is due to the fact that the tunnel is not straight and to the presence of the ventilation shafts. Depending on whether air is pushed through with a positive pressure gradient or pulled out with a negative pressure gradient, the shafts are either extracting or ingesting air. This, in turn, influences the velocity distribution in the bend. Average velocities in each section between the two ends and the shafts are shown in Fig. 10 below.

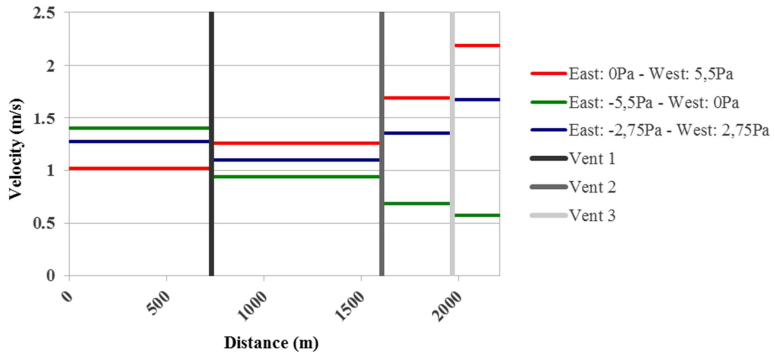

Figure 10: Natural ventilation. Average velocities for different pressure boundaries.

The velocities in the tunnel are bounded by the two extremes for cases 1 and 3. This is why these two methods were chosen when adding natural ventilation to the forced ventilation calculations.

5.2 Parametric Study

The parametric study was conducted on the different train models and tunnel surface roughness.

Detailed analysis of the flow field obtained with the detailed train model and tunnel surface roughness reveals significant wakes, flow recirculations and detachment due to the interaction between the main flow and the cars, and between the forced ventilation flow and the cars (Figs. 11, 12). The largest wakes are found at the end of each train.

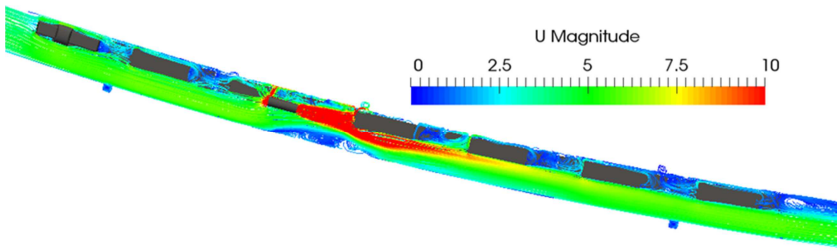

Figure 11: Detailed train model. Velocity magnitude – Train 1.

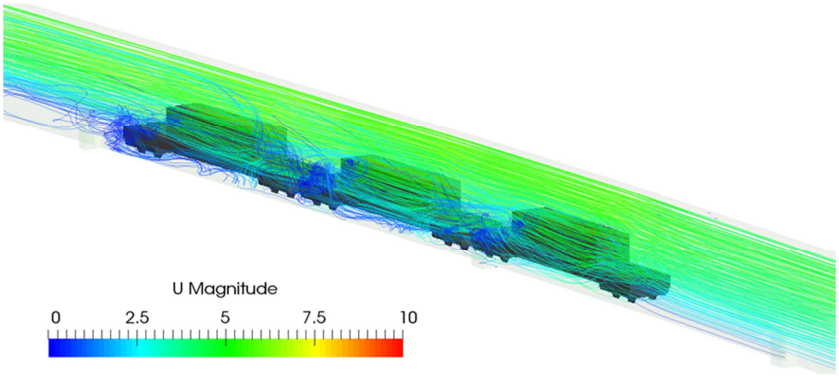

Figure 12: Detailed train. Streamlines coloured by velocity magnitude. Train 2.

Significant interaction between the wakes of the cars and the loads downstream are also observed. For train 4, the flow from the ventilation fan gives rise to a recirculation zone at the top of the car downstream of the fan (Fig. 13).

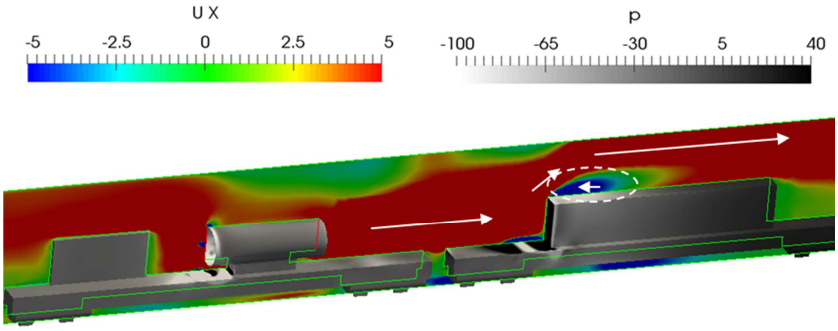

Figure 13: Velocity in the axial direction and pressure in a plane cutting through the centre of train 4.

Globally, the flow is highly non uniform in the axial and cross directions near and around the trains, which act as obstacles, and then becomes gradually more uniform away from the trains.

Plotting the average velocity in the tunnel sections shows that, compared to the natural ventilation models (Fig. 10), the velocities in the tunnel are about twice as large (Fig. 14).

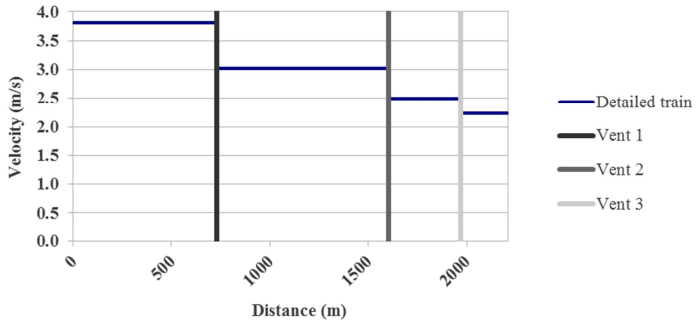

Figure 14: Detail train model. Average velocity in the tunnel.

To further evaluate the influence natural ventilation could have locally if it were directed opposite the forced ventilation flow, two additional cases were also run, imposing counter pressure gradients similar to those used in Section 5.1. The results show that the resulting mean velocity is almost the same in the sections near the trains. However, further away and closer to the exit, past the third ventilation shaft, the mean velocity is slower, which is consistent with additional flow leaving through the ventilation shaft.

When the train model is simplified to a tubular shape, strong and longer recirculation loops are observed along the tunnel near the ventilation fans (Fig. 15).

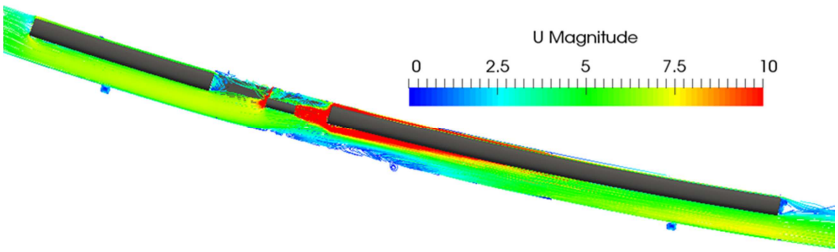

Figure 15: Tubular train model. Velocity contours. Train 1.

However, compared to the detailed train model, the reduction in wakes due to the absence of cars, bogies, and loads leads to an overall increase of 12-13% in mean velocities throughout the tunnel.

For the last comparison, the tunnel surface roughness is neglected. As shown in Fig. 16 below, with smooth walls the average velocities increase significantly, the effect being strongest further away from the trains and the fans. Similar to the observations when natural ventilation is taken into account with the detailed train, forced ventilation dominates the flow field nearer the trains and the effects of other parameters are more significant further away.

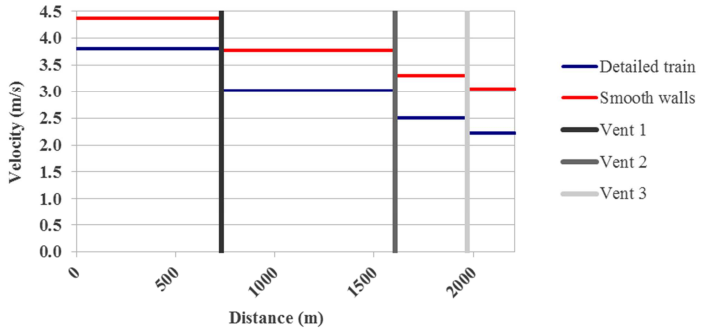

Figure 16: Detailed train model (rough and smooth tunnel walls). Average velocity.

To evaluate the different models and compare their results to the experimental data, similar to the measurements, mean values between the minimum and maximum values at each measuring section were calculated and plotted for each model (Fig. 17).

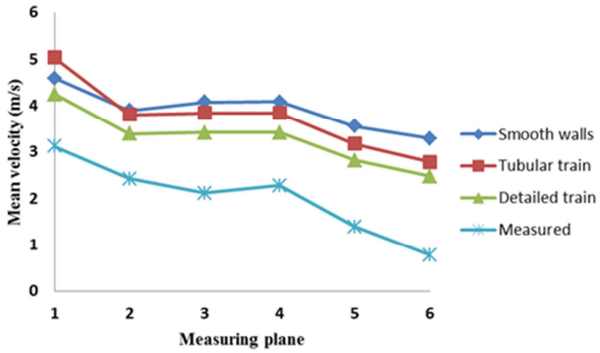

Fig. 17: Mean velocity at each measuring plane for the experiments and the different CFD models.

All the numerical results correctly reproduce the overall trend observed in the experiments, with step decreases in velocity for each section between the ventilation shafts.

Comparing the results for the tubular train, detailed train, and without surface roughness shows that both the train shape and the surface roughness have a significant influence on the calculated mean ventilation velocities. In the first section of the tunnel, between planes 1 and 2 where the building trains are situated, the influence of train shape is more significant than the tunnel surface roughness. Further away, towards the West end of the tunnel, the influence of surface roughness is more significant than the train shape.

Of these three models, the results with the detailed train and tunnel surface roughness agree best with the experimental results. However, all the models yield large overestimations of the mean velocity, compared to the measured values.

5.3 Reduced fan power

Since the detailed train model with tunnel surface roughness yielded average velocity distributions qualitatively similar to the measured values, and the fan settings the night of the measurements were unknown, an additional model was run where the fans were only powered at 70% of their nominal power. This could represent practical scenarios where they may have been intentionally or unintentionally turned down on the night of the measurements by the operators or, for example, fans degradation with age.

A very good agreement was then obtained, up to measuring planes 5 and 6 nearer the exit of the tunnel (Fig. 18).

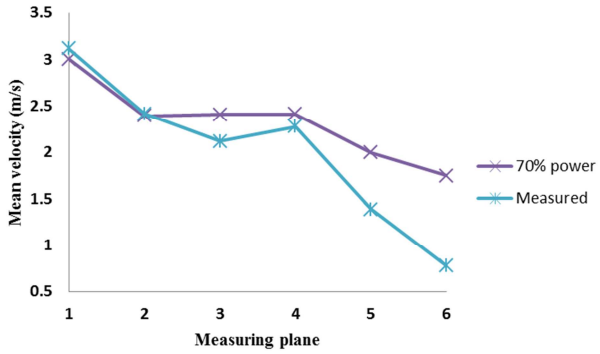

Fig. 18: Mean velocity at each measuring plane for the experiments and the reduced fan power CFD model.

To evaluate the accuracy of the CFD model in 3D, the relative error on the velocity was also computed at each measuring point in each measuring plane for this model (Fig. 19).

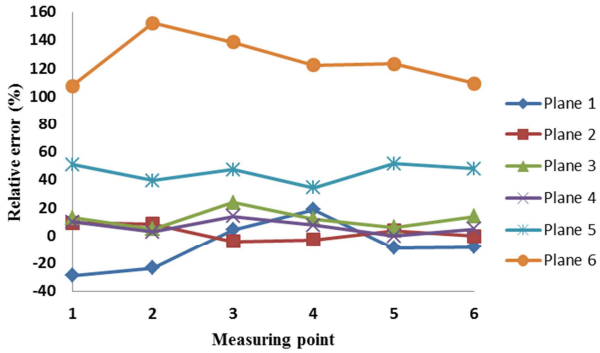

Figure 19: Reduced power CFD model. Error relative to the measured values, calculated at each measuring point of each measuring plane.

The results show that, with the reduced fan power, the relative error on the predicted velocity compared to the measured velocity is between -4% and 14% for measuring planes 1 to 4. It then increases to 44 and 125% nearer the tunnel exit, for planes 5 and 6. Whilst the velocities are predicted with good accuracy in the works area and downstream

of the trains up to the second ventilation shaft, the models are not able to predict the velocities in the last two sections of the tunnel. This area appears to be dominated by natural ventilation flow.

6 CONCLUSION

A series of velocity measurements was carried out in an SNCF Réseau rail tunnel during construction work in order to be utilised for validation of CFD models and to help start to define recommendations for CFD modelling of such complex tunnels and works configurations. The parametric CFD study examined the influence of train shape, surface roughness and ventilation settings, natural and forced. Best results were obtained with a detailed representation of trains broken down in their main components and accounting for the actual material of the tunnel surface. When the fan power settings were adjusted to 70% of their nominal value, good agreement was obtained between the numerical and experimental values in 3D near the trains and up to a work site length downstream of the trains. This indicates that a reliable 3D CFD model could be built on this basis for further modelling of smoke and dust dispersion, since good accuracy can be obtained in the work areas. However, it also highlights the importance of the fan settings during the works, which could not be verified since they had not been measured during the test campaign. Future measurement protocols will need to include this data and the CFD calculations can also be used as a tool to demonstrate the significance of the fan settings to operators. The CFD results also show that, whilst for the forced ventilation used in this tunnel natural ventilation is not significant nearer the trains, it plays a role away from the fans. Further work will be required to obtain good agreement between numerical and experimental values throughout the entire length of the tunnel by better capturing natural ventilation. To this end, in future studies it would be interesting to model the tunnel together with the surrounding volume around the tunnel and to take into account actual wind conditions.

REFERENCES

(1) I.E Idel'cik, *Memento des pertes de charge*. Eyrolles, EDF eds, Third ed, 1986.
(2) CETU, *Ventilation. Les dossiers pilotes du CETU*, Centre d'Etudes des Tunnels, www.cetu.gouv.fr, IBSN 2-11-084740-9, Nov. 2003.
(3) P. Thiaudière, Y. Chamerois, *Surveillance et maintenance des tunnels ferroviaires. Les apports des applications numériques. Monitoring and maintenance of rail tunnels. The benefits of digital applications*, Tunnels et Espaces Souterrains. No 257. Sept/Oct. 2016.
(4) AFTES, *Ventilation des ouvrages souterrains en cours de construction,* Recommandations de l'AFTES, GT27R1F1, 2003.
(5) C. Norris, A. Mercusot, P. Oriez, *Mechanical Ventilation of Underground Construction Works*, WTC16, San Franciso, USA, 2016.
(6) E. Béraud, Y. Chamerois, *La ventilation en chantiers ferroviaires souterrains. Applicabilité et adaptation des règles de l'art relatives aux ouvrages souterrains en cours de construction au cas des chantiers ferroviaires souterrains. Ventilation for underground rail worksites. Applicability and adaptation of best professional practice for underground structures under construction to underground rail worksites*, Tunnels et Espaces Souterrains, No 252, Nov/Dec 2015.
(7) SALOME, The Open Source Integration Platform for Numerical Simulation, www.salome-platform.org
(8) OpenFOAM, openfoam.org
(9) ParaView, www.paraview.org